ARCTIC
VOL. 70, NO. 4 (DECEMBER 2017) P. 389–402
https://doi.org/10.14430/arctic4685

Episodic and Systematic Tree Ring-Width Variation (AD 1763–2013) in the Takhini Valley, Southwest Yukon, Canada

Wayne L Strong[1]

(*Received 26 May 2017; accepted in revised form 29 August 2017*)

ABSTRACT. A tree-ring analysis of 764 western white spruce (*Picea albertiana*) in the Takhini Valley of southwest Yukon was conducted to assess short- and long-term variation in growth and local climate. The resulting chronology spanned the period from AD 1763 to 2013. A polynomial regression ($R = 0.720$, $p < 0.001$) indicated that the pre-1840 segment of the chronology had below-normal tree ring-width index (RWI) values (average 0.64, with modest variation), but the subsequent segment had greater variation and a steady increase in RWI values (average 0.89) until ~1920. After 1930, RWI values began to increase again (average 1.06) with 51% more variation than had previously occurred. Peak RWI values after 1930 were double those of the early 1800s. RWI values were uncorrelated with air temperature variables (except September minima), but weakly and positively correlated ($r < 0.35$) with precipitation variables. RWI values were moderately correlated with annual heat-moisture index values ($r = -0.415$, $p < 0.001$), although more strongly with RWI values less than 1.1 ($R = -0.631$, $p < 0.001$). Therefore, the RWI chronology was interpreted from an ecological moisture-balance perspective, with possible long-term temperature changes estimated from archival sources. The latter suggested a 2.1˚–3.1˚C rise since the early 1800s. Extreme RWI values and portions of the chronology were associated with known environmental events.

Key words: dendrochronology; climate; forest history; moisture; palaeoclimate; ring-width; white spruce; Yukon

RÉSUMÉ. L'analyse des anneaux de croissance de 764 épinettes blanches de l'Ouest (*Picea albertiana*) de la vallée Takhini, dans le sud-ouest du Yukon, a été effectuée dans le but d'évaluer les variations à court et à long termes en matière de croissance et de climat local. La chronologie qui en a découlé s'étend sur la période allant de 1763 à 2013 de notre ère. La régression polynomiale ($R = 0{,}720$, $p < 0{,}001$) a permis de déterminer que les valeurs des largeurs d'anneaux de croissance du segment chronologique précédant 1840 étaient en bas de la normale (moyenne de 0,64, avec de modestes variations), mais que les valeurs des largeurs d'anneaux du segment subséquent affichaient de plus grandes variations et une augmentation continue des valeurs des largeurs d'anneaux de croissance (moyenne de 0,89) jusque vers 1920. Après 1930, ces valeurs ont recommencé à augmenter (moyenne de 1,06) pour afficher une variation 51 % plus élevée que celle enregistrée auparavant. Après 1930, les valeurs maximales des largeurs d'anneaux correspondaient au double de celles du début des années 1800. Les valeurs des largeurs d'anneaux n'ont pas été corrélées avec les variables des températures de l'air (à l'exception des minimums de septembre), mais ont fait l'objet d'une corrélation faible et positive ($r < 0{,}35$) avec les variables des précipitations. Les valeurs des largeurs d'anneaux de croissance ont fait l'objet d'une corrélation modérée avec les valeurs annuelles des indices de chaleur et d'humidité ($r = -0{,}415$, $p < 0{,}001$), et d'une corrélation plus forte avec les valeurs des largeurs d'anneaux de moins de 1,1 ($R = -0{,}631$, $p < 0{,}001$). Par conséquent, la chronologie des largeurs d'anneaux de croissance a été interprétée à partir de la perspective du bilan d'eau du sol et les changements possibles de températures à long terme ont été évalués à partir de sources archivées. Ces dernières ont permis de suggérer une augmentation de 2,1˚à 3,1 ˚C depuis le début des années 1800. Les valeurs extrêmes et les segments chronologiques des largeurs d'anneaux de croissance ont été associés à des événements environnementaux connus.

Mots clés : dendrochronologie; climat; histoire de la forêt; humidité; paléoclimat; largeur des anneaux de croissance; épinette blanche; Yukon

Traduit pour la revue *Arctic* par Nicole Giguère.

INTRODUCTION

The Intergovernmental Panel on Climate Change (IPCC, 2013:22) predicted a 1˚–1.5˚C to 4˚–5˚C increase in average annual temperature above the 1986–2005 level in the Canadian boreal forest by AD 2100. However, between 1956 and 2005, recorded temperatures increased 1.8˚C in Yukon (Streicker, 2016) and 2.7˚C at Whitehorse (Pinard, 2007) although the global increase was only 0.7˚C (IPCC, 2013). Part of the differential between the global and Yukon increases was likely due to more rapid warming at high latitudes than at low latitudes. Although temperatures

[1] Arctic Institute of North America, 2500 University Drive NW, Calgary, Alberta T2N 1N4, Canada; and Yukon Research Centre, Yukon College, 500 College Drive, PO Box 2799, Whitehorse, Yukon Y1A 5K4, Canada; wstrong@yukoncollege.yk.ca

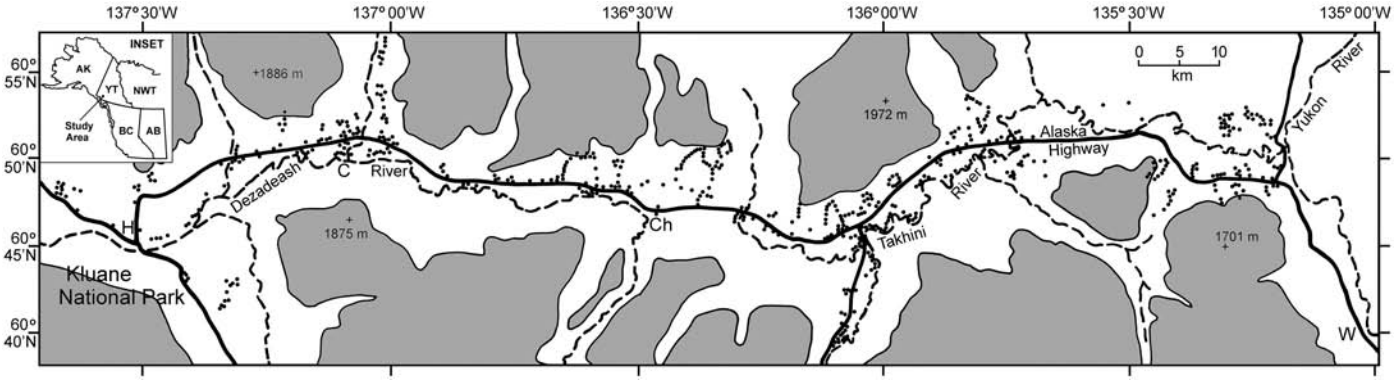

FIG. 1. Distribution of trees used to construct the ring chronology relative to elevations in the Takhini Valley of southwest Yukon. A dot indicates the location of one or more trees. Shading represents areas above 1000 m, with valley bottom elevations ranging from 600 to 700 m. See inset for location of study area within northwestern North America: W – Whitehorse; C – Canyon; Ch – Champagne; H – Haines Junction; AB – Alberta; AK – Alaska; BC – British Columbia; NWT – Northwest Territories; and YT – Yukon.

are predicted to be warmer by the end of the 21st century, climate modeling indicates total annual precipitation will increase less than 10% above 1986–2005 levels in the Yukon region (IPCC, 2013:22). A rise in temperature without a corresponding increase in effective moisture could have a long-term effect on the physiognomy and botanical composition of the indigenous vegetation, as well as on conifer tree growth (m^3 ha^{-1} yr^{-1}) (Wang et al., 2006; Miyamoto et al., 2010; Griesbauer and Green, 2012). Changes in vegetation could in turn affect the composition and abundance of wildlife in the territory.

To understand how predicted 21st century climate warming might affect southern Yukon, it would be helpful to know how the local climate has varied during the past 200–300 years and what factors drove that variation. Unfortunately, we lack meteorological data to characterize conditions prior to 1940. Therefore, an indirect method such as tree-ring analysis would need to be employed to address these considerations. In Yukon, as well as elsewhere, tree-ring analyses typically involve obtaining growth-increment cores from 20–30 dominant trees in a stand with quasi-homogenous ecological conditions. Once these data are detrended to eliminate age-related growth in individual trees, the resulting ring-widths, after conversion to index values, form a temporal pattern that can represent climate variation. A spatial context is added to a tree-ring analysis by sampling more than one stand. Using these commonly applied procedures, the analysis of even a single stand can be labor-intensive, with the final sample size equal to the number of studied stands regardless of the number of analyzed tree-ring series.

If sampled stands are located in close proximity and have similar site conditions with a common history, a relatively consistent temporal trend of change can be anticipated. In the southwest Yukon region, however, tree-ring analysis stands are often 20–50 km apart (e.g., Davi et al., 2003; Chavardès et al., 2013) and sometimes even farther apart in individual studies (e.g., Youngblut and Luckman, 2008). When combined with an ecologically diverse landscape (Meidinger and Pojar, 1991; Strong, 2013) and complex mountain terrain, these separation distances raise the question of how comprehensive a temporal model can realistically be expected. Mountainous terrain in particular can have a substantial effect on tree growth because over short distances, temperatures and precipitation can vary spatially, vertically, and according to topographic position. From a practical perspective, it is often difficult to find stands with similar and appropriate site conditions that also have multiple older trees, particularly when the fire-return interval is relatively short (e.g., 90 ± 30 yr, Drury and Grissom, 2008). If we exclude methodological considerations, it is probably because of landscape diversity and the distance between sampled stands that, despite several dendrochronology studies in the southwest Yukon region, no common pattern of temporal change has emerged among completed tree-ring analyses (Allen, 1982; Davi et al., 2003; Zalatan and Gajewski, 2005; Youngblut and Luckman, 2008; Griesbauer and Green, 2012; Chavardès et al., 2013; Morimoto, 2015). Even in studies with relatively close stands (Zalatan and Gajewski, 2005; Chavardès et al., 2013), individual stand chronologies often lack common temporal patterns. In the Slims River Valley, near Kluane Lake in southwest Yukon (Allen, 1982), changes in tree-rings are actually the opposite of what would be expected, with ring-widths increasing as trees age.

To create a more spatially and temporally coherent portrait of changing tree-ring growth to interpret past climate change in southwest Yukon, we need either a much denser network of analyzed stands than currently exists or a different sampling approach. For the latter, an alternative might be to use a large number of individual trees that are scattered across a study area and occupy similar site conditions. The non-stand analysis approach is not new. It has been used for chronologies developed where trees are naturally of low density because of harsh environmental conditions (e.g., LaMarche, 1974; Grissino-Mayer et al., 1997; Yang et al., 2014; Chen et al., 2016) and where the sample consisted of building timbers and scattered dead trees (LaMarche, 1974; Speer, 2010; Prokop et al., 2016). The use of scattered trees or a semi-random sampling

TABLE 1. Average monthly and annual temperature and precipitation values at Whitehorse Airport from November 1941 to October 2013 (Environment Canada, 2016).

Month	Season	Average temperature (˚C) (SD)	Total precipitation (mm) (SD)
November	Winter	−9.3 (4.8)	21 (10)
December	Winter	−15.0 (5.8)	19 (11)
January	Winter	−17.8 (6.7)	18 (9)
February	Winter	−12.7 (5.0)	13 (8)
March	Winter	−7.4 (3.3)	13 (9)
April	Transitional	0.5 (2.2)	9 (8)
May	Summer	7.2 (1.3)	14 (10)
June	Summer	12.3 (1.5)	30 (19)
July	Summer	14.1 (1.1)	38 (19)
August	Summer	12.5 (1.4)	38 (21)
September	Summer	7.4 (1.4)	31 (15)
October	Transitional	0.6 (1.9)	22 (11)
	Annual	−0.6 (1.3)	265 (47)

design might also be less prone to systematic bias than the classic stand-based approach (Nehrbass-Ahles et al., 2014). The choice of approach can be either related to the study objectives and available resources, or largely philosophical, because both approaches can yield similar results (e.g., Fierke et al., 2005; Popovic and Menzies, 2006). The intensive sampling approach, however, can be constrained by the availability and the appropriate distribution of suitable stands within a study area, which seems to be an issue in parts of southwest Yukon. While extensive sampling can provide better spatial coverage, it is also likely to include greater variation and more anomalies than intensive sampling, because the latter involves within-stand averaging of tree-ring data. However, the importance of anomalies in the extensive sampling approach is minimized by the overall data response.

This study was based on a design that involves extensive tree sampling. Its objectives were to (1) construct an index-based tree-ring width chronology for the Takhini Valley of southwest Yukon, using western white spruce (*Picea albertiana* ssp. *albertiana* S. Brown emend. Strong & Hills (Strong and Hills, 2006), syn. *Picea glauca* (Voss) Moench × *engelmannii* Parry ex Engelmann) that occur at low elevations and on climatically sensitive sites (sensu Speer, 2010); (2) identify short-term patterns and the long-term temporal trend of tree-ring index values; and (3) relate tree-ring index values to local meteorological parameters and historical environmental events as a basis for interpreting and in part validating the chronology.

MATERIALS AND METHODS

Study Area

The study area included the valley bottom to mid-elevation slopes of the Takhini Valley, which is the largest east-west valley in southwest Yukon (60˚–62˚ N, 135˚–141˚ W). The study area extended ~135 km westward from the confluence of the Takhini and Yukon Rivers to the eastern boundary of Kluane National Park and was 7–10 km wide along much of its extent (Fig. 1). Valley bottom elevations ranged from 600–700 m, with the higher elevations forming the drainage divide between the Takhini and Dezadeash basins near 136˚20′ W longitude (Fig. 1).

The lower elevations of the Takhini Valley area have an annual average temperature of −0.6˚C according to meteorological data for 1942–2013 collected at Whitehorse Airport (station 2101300) (Environment Canada, 2016). Average monthly temperatures warmer than 5˚C (summer) occur from May to September (average 10.7˚C, SD = 0.8), with a peak in July (Table 1). The 5˚C temperature threshold is important because monthly averages of 4˚–5˚C approximate the minimum temperature needed to initiate ring development in conifers (Rossi et al., 2008). Winters or months with mean temperatures of −5˚C or lower (November–March) averaged −12.4˚C (SD = 2.4). April and October were considered transitional months. About half of the annual precipitation falls from June to September (137 mm), with most rainfall in July and August. April is the driest month (Table 1). Regionally, the Takhini Valley is semi-arid (Jätzold, 2000) because it occurs in the rain shadow of the St. Elias Mountains. Regression analysis indicates that between 1943 and 2013, summer and annual temperatures had modest but significant ($p < 0.05$) patterns of temporal change (Fig. 2A). The summer temperature trend-line peaked at both ends of the time frame, whereas annual temperatures were highest in the early 1940s and early 2000s. Neither precipitation (Fig. 2B) nor heat-moisture index values (Fig. 2C) contained statistically significant summer or annual patterns of change.

Low to middle elevations in the Takhini Valley are part of the Mid-Cordilleran Boreal ecoclimatic region (Strong, 2013). Seral forests in the eastern one-third of the valley include lodgepole pine (*Pinus contorta* var. *latifolia* Engelmann ex S. Watson) and to a much lesser extent trembling aspen (*Populus tremuloides* Michx.), whereas in the western portion of the study area, western white spruce predominate. Correspondingly, the eastern stands tend to be 50–60 years old, whereas those farther west are often at least 60 to 120 years old. Ecologically, western white spruce form stands (e.g., 30%–40% canopy cover) on sites

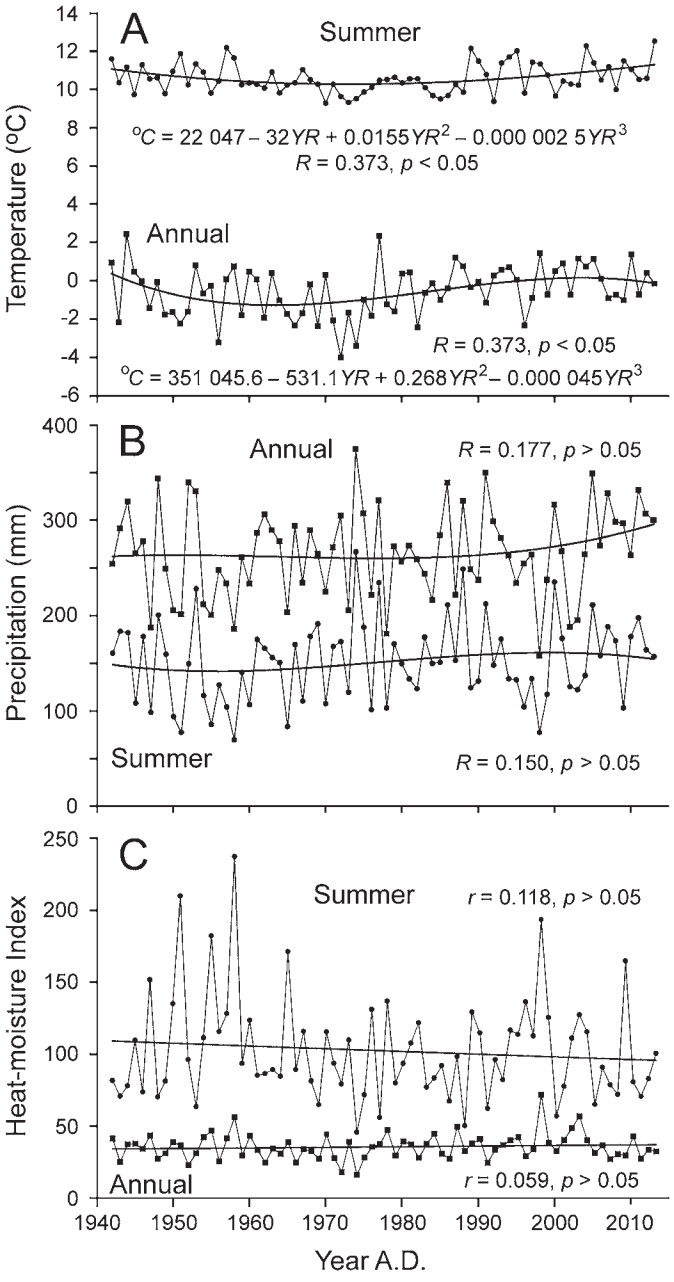

FIG. 2. Annual and summer temperatures (A), precipitation (B), and heat-moisture index values (C) for Whitehorse Airport, Yukon. Lines represent simple or polynomial regression trend lines. In the temperature equations, the variable YR is calendar year. Temperature and precipitation data were from Environment Canada (2016).

with conditions ranging from xeric to subhygric. Because of their greater height-growth potential (20–25 m), spruce can quickly become dominant trees in juvenile forest stands (12–15 m). Wildfires play an important role in forest dynamics throughout the valley, although major events are infrequent. Spruce bark beetle (*Dendroctonus rufipennis* Kirby) has also caused substantial spruce mortality in the western portion of the study area since the early 1990s. Native vegetation is common because human activity has been minimal, but both land clearance for agriculture and forest harvesting are becoming more common. For the latter, firewood collection and commercial logging are typically limited to small areas with road access.

Tree Core Collection and Processing

Possible areas with older spruce were identified using aerial photography and unpublished 2009 1:50 000-scale forest cover maps from Yukon Energy, Mines and Resources. Suitable trees for growth increment coring were subsequently sought through reconnaissance trips into the candidate areas from mid-September through October 2013 and late April through June 2014. Throughout the study area, trees considered suitable for coring were located on well-drained sites that were dependent upon precipitation as their sole moisture source; that is, they lacked other sources of moisture such as a water table or overbank stream flow. Cored trees were located on level sites and on south-facing slopes (overall range of compass orientations: 110˚–260˚), where they were exposed to the direct effects of solar radiation. Exclusion of north-facing slopes and shaded areas avoided sites with greater potential for effective moisture availability and lesser physiological transpiration demand than were characteristic of the regional climatic regime, which could affect the amount and response pattern of tree-ring growth. The trees included in the sample represented chance encounters. Cored trees had a normal growth-form and lacked overt evidence of past physical damage. Some standing dead trees were cored to bolster the number of older spruce from the western one-third of the study area, where logging and a mid-1990s to mid-2000s spruce bark beetle outbreak reduced the number of live older trees. Because spruce bark beetles kill trees within 24 months of infection (Yukon Forest Management Branch, 2010), they had no effect on pre-infection ring growth.

Growth-increment coring (4.5 mm diameter) focused on more mature and larger western white spruce, but they were not necessarily old-growth trees. Often, only a single individual was available for coring on a site. To facilitate the collection of samples throughout the study area, coring was typically limited to trees at least 100 m apart. Exceptions to this arbitrary distance were made when older nearby trees occurred on different topography (e.g., hillcrest versus an adjacent steep slope) that offered the possibility of different climatic responses. Coring was done at a height of 130 (± 70) cm. This coring height avoided the small ring-widths caused by understory vegetation competition during the early years of tree growth. Locations on tree stems where branches might distort ring formation were also avoided. Because asymmetrical stem growth often occurred, only the longest and best-quality core among extractions from an individual tree was retained for analysis. Although two cores per tree are suggested to account for within-tree variation in growth (Speer, 2010), use of a single core is not an uncommon practice (e.g., Griesbauer and Green, 2012; Chavardès et al., 2013; Lloyd et al., 2013). It was assumed that relative interannual variation in ring growth was similar along different stem radii, although the

absolute amount of ring growth varied (Speer, 2010). After extraction, individual cores were wrapped in paper and air-dried.

Ring-Width Measurement and Standardization

Post-field processing of cores involved conventional mounting and sanding (Speer, 2010), but was followed by gray-scale digitizing at 945 pixels cm^{-1} using a flatbed scanner (similar to commercial tree-ring analysis systems such as WinDendroTM or CooRecorder). Scanned cores were imported into Adobe Photoshop® Elements 4.0 software and enlarged 83×, to a size that just filled the vertical view of a 30 cm high flat-screen computer monitor with the width of the core. The beginning of each growth ring was marked with a pixel, and individual rings were numbered on the digital image before manual measurement. Prior to analysis, enlarged ring measurements were converted to actual widths (mm). Seven marker rings that had reduced ring-widths (1807, 1834, 1889, 1916, 1958, 1978, and 1998) and 2013 were used to manually cross-date ring series using Microsoft EXCEL software. This cross-dating procedure was a computer spreadsheet version of the Yamaguchi (1991) method. The results were reviewed using COFECHA software (March 2014 version, http://www.ldeo.columbia.edu/tree-ring-laboratory/resources/software) to identify possible errors and inconsistencies.

The Signal-Free Multiple Regional Curve Standardization (SF-MRCS) method was used to standardize tree-ring series and to preserve long-term low-frequency trends (D'Arrigo et al., 2006; Melvin and Briffa, 2014a). Several Regional Curve Standardization (RCS) curves were developed by aggregating ring series with similar temporal growth patterns and levels of peak growth. RCS curves that included fewer than 30 series were removed from consideration. Climatic Research Unit Standardisation of Tree-ring data (CRUST) software (Melvin and Briffa, 2014a) was used to calculate tree ring-width index (RWI) values for each RCS curve, which resulted in a temporal sequence of standardized RWI values for each curve. Because multiple RCS curves were used to create the final or master chronology, individual RWI curves are referred to as sub-chronologies. RWI values were calculated using the ratio between measured and expected ring-widths, with sub-chronology means set to 1.0. The RCS sub-chronologies were developed by arithmetic averaging of yearly RWI values, because averages and robust means produced essentially the same result, and robust means are considered effective only when the sample size includes 10–20 series (Melvin and Briffa, 2013:5). The normality of RWI values was assessed using Kolmogorov-Smirnov tests. Compilation of the final or master chronology for the Takhini Valley was based on averaged sub-chronologies, because the dataset exceeded the "40 trees per RCS curve with a maximum of 11 RCS curves" capacity of the CRUST software (Melvin and Briffa, 2013:9). Averaging assumed that each RCS sub-chronology represented an independent temporal estimate.

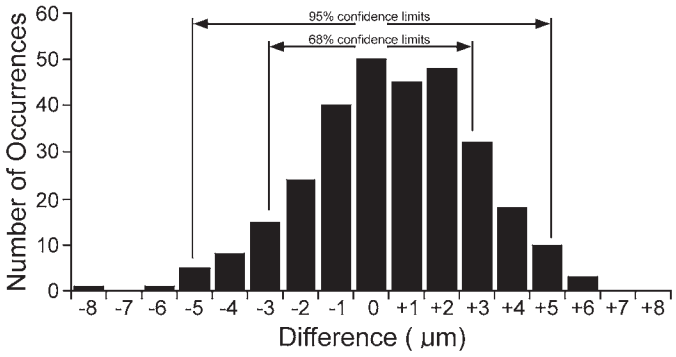

FIG. 3. Accuracy estimate for tree ring-width measurement method based on differences between actual and measured distances with associated confidence intervals (n = 300).

Interannual variation in RWI values was generalized using three-point moving averages, whereas the long-term trend was characterized using polynomial regression (R).

Series intercorrelation and average mean sensitivity (acceptable range 0.1–0.4, Speer, 2010) for RCS sub-chronologies and the master chronology were determined using COFECHA. RCS-based expressed population signal values (EPS_{RCS}, Melvin and Briffa, 2014b) for the master chronology were derived from a simultaneous analysis of all RWI series used in the analysis (acceptable limit 0.85, Speer, 2010). Kruskal-Wallis and nonparametric Scheffé rank (α = 0.05 level, Miller, 1966: formula 110) tests were used to evaluate differences in spatial distribution and general site conditions among the trees that formed different RCS curves.

Accuracy of Ring Measurements

Because ring-widths were measured using hardware and software not specifically designed for the purpose, accuracy of the ring-width measurement method was assessed on the basis of differences (d_i) between actual (a_i) and measured (m_i) distances. Actual values were determined by calculating the distance between two divergent lines that were separated by 5 mm at 100 cm: $a_i = b_i /100 \times 5$, where b represents the distance from the convergence point of the two lines to the measurement point. The 5 mm separation distance incorporated 99.97% of all measured Takhini Valley rings. Locations for calculating a_i and measuring m_i were based on 300 randomly generated numbers (i = 1, ..., 300) between 0 and 300. Distances between lines were measured perpendicular to the base line after enlarging the measurement model 83×. The error (µm) between distances was determined as follows: $d_i = (m_i - a_i /83) \times 1000$. A negative d_i represented an underestimation.

Maximum d_i typically occurred ± 6 µm (SD = 2.4) of the actual distance (Fig. 3), which was less than the 10 µm measurement accuracy reported in other recent studies (e.g., Flower and Smith, 2011; Szymczak et al., 2014; Prokop et al., 2016). A near-perfect positive correlation (r > 0.999) occurred between a_i and m_i values, with a 2.4 µm regression

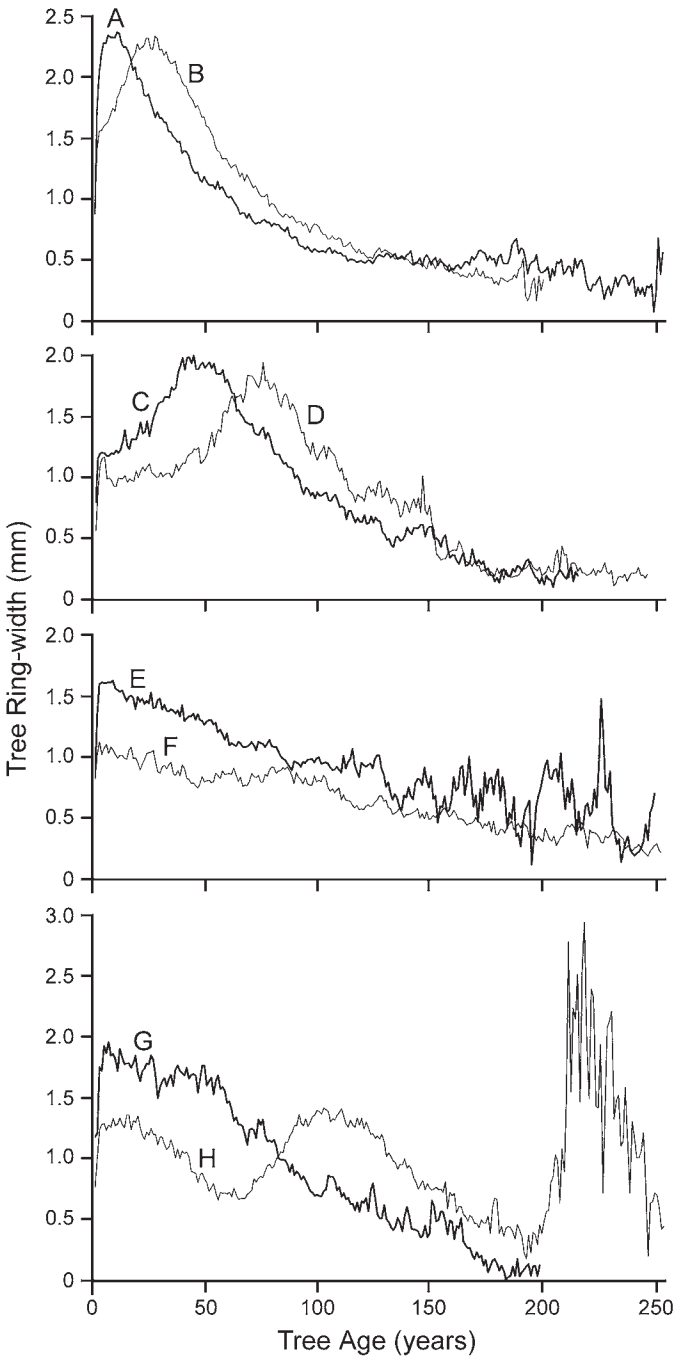

FIG. 4. Eight (A–H) common Regional Curve Standardization (RCS) growth models in the Takhini Valley based on annual western white spruce ring-widths (mm). Year 0 is the stem pith. RCS models included 38–213 tree-ring series (Table 2).

standard error of estimate (SEE), which corresponded to 95% confidence limits of ± 4.7 μm (Fig. 3). In comparison, Schmidt et al. (1996:869) considered a 6.2 μm SEE to represent a "very low error" level.

Climate Data Analysis

Meteorological data were reviewed for four stations located within and near the Takhini Valley (Environment Canada, 2016). The records for three stations were considered too fragmented to be reliable (Haines Junction) or too short to be useful (Otter Falls and Takhini River Ranch). The Whitehorse Airport station (Fig. 1) had the longest available record, with 48 months missing one or more maximum or minimum temperatures or precipitation measurements in a dataset of 864 months (1942–2013). No other meteorological record of greater length occurred within 200 km of the Takhini Valley. Missing record values were estimated to maximize the usefulness of the existing meteorological record. If four or fewer daily values were missing for a parameter and the gaps were only a day in length, the missing numbers were estimated by averaging adjacent daily values. If more daily values were missing, they were estimated from other stations that occurred near the Whitehorse Airport (Nos. 2101310, 2101400, or 2101290), using regression analysis to adjust for systematic differences.

Maximum, minimum, and mean temperatures and precipitation on an annual, monthly, and summer basis were compiled for climate interpretation and reconstruction purposes (56 variables). Early growing-season months (May–June, May–July, and June–July) were calculated for the same variables (12 variables). To assess climatic moisture balances within the study, annual (AHMI = [mean annual temperature (˚C) + 10]/[mean annual precipitation (mm)/1000]) and summer heat-moisture index values (SHMI = mean warmest month (˚C)/[mean summer precipitation (mm)/1000]) were calculated (Wang et al., 2006). In addition, potential moisture deficits (i.e., precipitation minus potential evapotranspiration, P − PE) with day-length adjustments (Thornthwaite, 1948) were compiled for annual, summer, and monthly (May–September) periods, and for May–June, May–July, and June–July. Zero represented a balanced relationship for these three indices. Larger HMI and more negative P − PE values indicated greater moisture deficits. November was used as the beginning of a new climate year, so all winter months were chronologically sequential and represented conditions that occurred prior to a growing season.

Pearson product-moment correlation (r) was used to determine the strength and the nature of the relationship between RWI values and climate variables, whereas regression was used to illustrate numerical relationships.

RESULTS

Characteristics of the Tree-Ring Dataset

A total of 838 tree-ring series occurred in the Takhini Valley dataset. Trees were scattered throughout the length of the study areas, but only north of the Takhini and Dezadeash Rivers and west of the Alaska Highway crossing of the Takhini River (Fig. 1). Cored trees occurred at elevations ranging from 611 to 1125 m (average 755 m, SD = 88). Most trees (90%) were more than 98 m apart,

TABLE 2. Characteristics of Regional Curve Standardization (RCS) tree-ring growth models (cf. Fig. 4).

RCS curve	Number of series	First year	Last year	Record length (years)	Mean sensitivity	Series intercorrelation
A	185	1760	2013	254	0.288	0.647
B	213	1817	2013	197	0.273	0.687
C	83	1799	2013	215	0.260	0.664
D	64	1767	2013	247	0.278	0.622
E	76	1832	2013	182	0.291	0.702
F	46	1726	2013	288	0.271	0.588
G	38	1817	2013	197	0.264	0.639
H	59	1736	2013	278	0.290	0.624
All	764	1726	2013	288	0.278	0.658

with 75% at distances of more than 228 m. Judging on the basis of 381 tree-rings and 12 years of growth to reach coring height, the oldest tree germinated about AD 1621, and the dataset included individuals as young as 50 years old. Spruce bark beetles killed less than 3% of cored trees. Fewer than five of the outermost rings in these series were removed from consideration because of beetle effects and surface decay due to weathering that rendered them unusable. Larger tree-rings bracketed ~86% of the 3674 marker ring comparisons resulting from cross-dating, with smaller rings bracketing under 2%. On average, an individual series included 125 rings. Average ring width was 1.179 mm (SD = 0.73), and 95% of rings were more than 0.258 mm wide.

RCS Curves

Eight distinctive RCS curves were recognized in the tree-ring dataset (Fig. 4). These curves incorporated 764 of the available ring series. The remaining series occurred in six RCS groupings with 5–15 members (n = 51) or were unclassified (n = 23). RCS curves A and B comprised more than half of the 764 series (Table 2). Curves A–D represented a sequence that had progressively less maximum annual growth, which occurred progressively later in the life of the associated trees. Peak growth in curve A averaged 2.35–2.40 mm yr^{1} during years 7–11 (Fig. 4). Annual ring-growth in the G, E, and F curves had maxima of ~1.8, 1.6, and 1.1 mm in the ninth year, respectively, with annual growth declining with age. RCS curve H had an abnormal shape due to three periods of elevated growth. In this curve, rings more than 200 years old were represented by a single ring series. Kruskal-Wallis and nonparametric Scheffé rank testing identified no significant differences among the trees that formed the different RCS curves, with respect to UTM Easting, elevation, slope orientation, or slope gradient.

The RCS curves had record lengths of 182–288 years (Table 2). Mean sensitivity among curves was similar and near the mid-range of acceptability. Series intercorrelation ranged from 0.62 to 0.70, except that curve F was slightly less. EPS_{RCS} equal to 0.85 or more occurred after 1810, faltered from 1815 to 1818 (minimum 0.81), then again exceeded 0.85 (Fig. 5B). Kolmogorov-Smirnov testing of yearly sets of values indicated that skewing of RWI values was not an issue.

Despite development by different growth patterns (Fig. 4), RCS sub-chronologies were very similar from 1810 to 2013 (Fig. 5A). Chronology patterns were more erratic before 1810, particularly the H sub-chronology (i.e., the lowest curve). Only 5–16 ring series occurred in the pre-1811 portions of these four RCS sub-chronologies, whereas more than 16 series occurred after 1810, and more than 50 by 1834 (Fig. 5C).

Takhini Valley Master Chronology

The Takhini Valley SF-MRCS master chronology was 251 years long and extended from 1763 to 2013 (Fig. 5B). The chronology consists of three broadly different segments based on different patterns of RWI variation: pre-1840 (77 years); 1840–1930 (90 years); and post-1930 (83 years). Prior to 1840, RWI values averaged 0.64 (SD = 0.10), with lows of ~0.47 from 1807 to 1817 (Fig. 5B). Few post-1840 RWI values deviated to the lows that occurred in the first segment. RWI values during the 1840–1930 period averaged 0.89 (SD = 0.14), included more years with values greater than 1.0, and had more variation than during the previous segment. If not for an abrupt reduction in growth from 1844 to 1846 and a prolonged reduction from 1877 to 1889 (Fig. 5B), variance of the first and second segments of the chronology would have been more similar. RWI values less than 1.0 became more frequent (14 occurrences) during the last 40 years of the second segment. After 1930, the average RWI value (1.06) was greater and the variability substantially more (SD = 0.24) than during either of the two other segments. The third chronology segment consisted of a distinct cyclic pattern that included four prominent periods of above-normal growth, with two distinct and one subdued period of below-normal RWI values (Fig. 5B). Maximum RWI values typically ranged from about 1.3 to 1.4. The range in RWI values during the third segment of the chronology was 51% greater than during the previous 168 years (0.77), with an average range in RWI values of 1.16.

A four-order polynomial regression indicated that RWI values on average steadily increased from ~1790 to ~1920, when values reached a short-lived plateau (Fig. 5B). After 1930, RWI values began to increase again. The regression model explained 52% of the temporal variance in RWI values (R = 0.720, $p < 0.001$, n = 251).

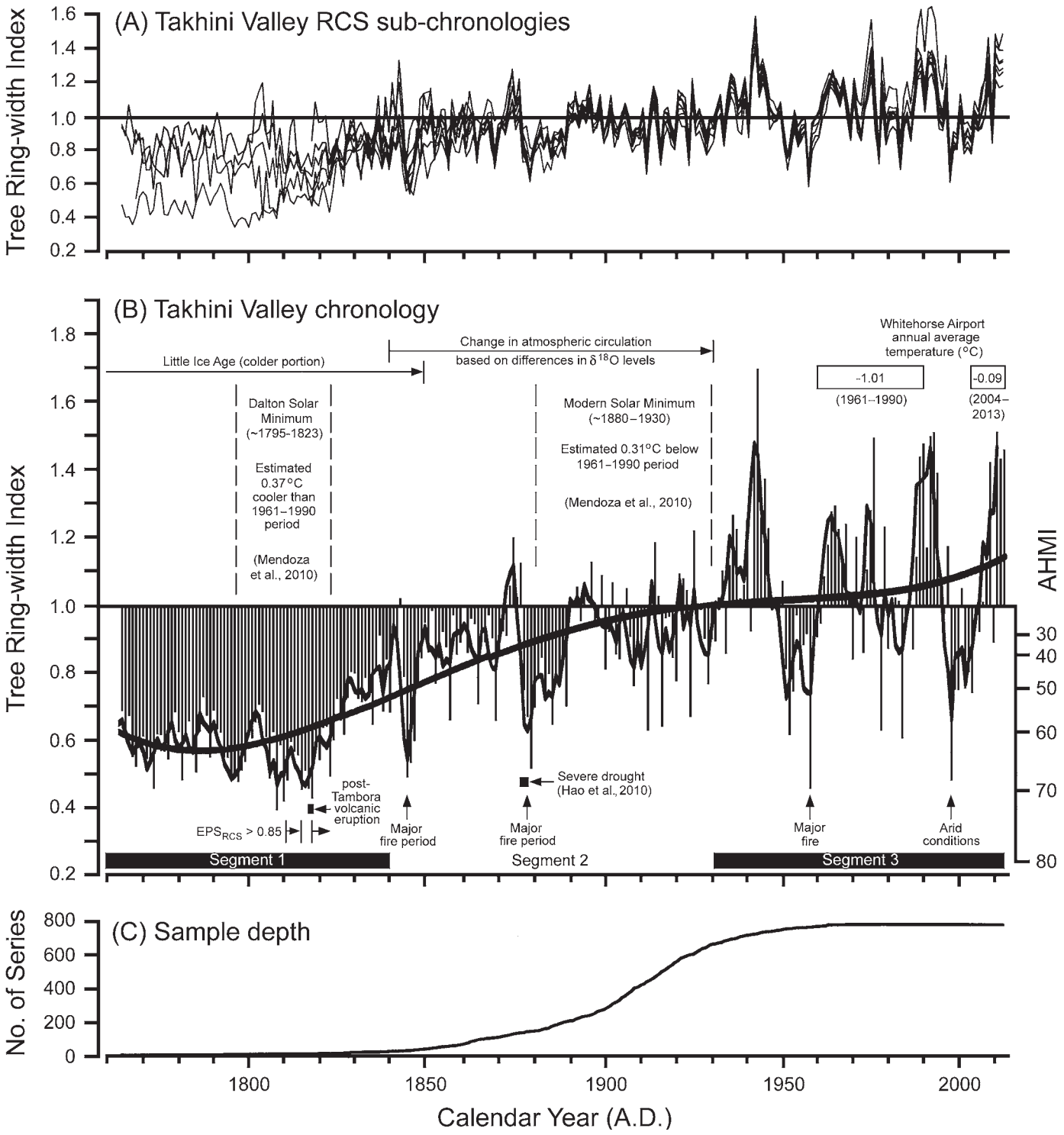

FIG. 5. Takhini Valley tree ring-width index chronology (B) with annual values (vertical bars) as derived from Signal-Free Multiple Regional Curve Standardization (SF-MRCS), with short-term (undulating line based on three-point moving averages) and long-term (sinuous line based on a fourth-order polynomial regression, $R = 0.720$, $R^2 = 0.518$, $n = 251$, $p < 0.001$) temporal trends for AD 1763–2013. An index value of 1.0 represents average growth. Also included are (A) the eight RCS sub-chronologies used to construct the SF-MRCS chronology and (C) the sample depth associated with the chronology. The annual heat-moisture index (AHMI) scale was based on the regression model presented in Figure 6.

Climate Variables and Tree-Ring Growth

Of 78 considered climate variables, only 10 were significantly ($p < 0.05$) correlated with 1942–2013 RWI values, and none were strongly correlated (Table 3). Except September minimum temperatures, all significant correlations were related to precipitation and moisture availability (Table 3). The strongest RWI correlations occurred with annual total precipitation and annual heat-moisture index (AHMI) values (Table 3), with the

TABLE 3. Correlation coefficients (*r*) between Takhini Valley Signal-Free Multiple Regional Curve Standardization tree ring-width index (RWI) values and Whitehorse Airport meteorological values ($n = 72$).

Climate variable (1942–2013)[1]	*r*-value	*p*-value
September minimum temperature (˚C)	0.266	0.024
Annual total precipitation (mm)	0.341	0.003
June–July precipitation (mm)	0.262	0.026
July precipitation (mm)	0.267	0.024
May–June P − PE (mm)	-0.258	0.028
May–July P − PE (mm)	0.247	0.036
June–July P − PE (mm)	0.289	0.014
July P − PE (mm)	0.281	0.017
Summer heat-moisture index	−0.286	0.015
Annual heat-moisture index	−0.415	< 0.001

[1] See Climate Data Analysis section in Materials and Methods for 68 other tested but statistically insignificant ($p > 0.05$) climate variables.

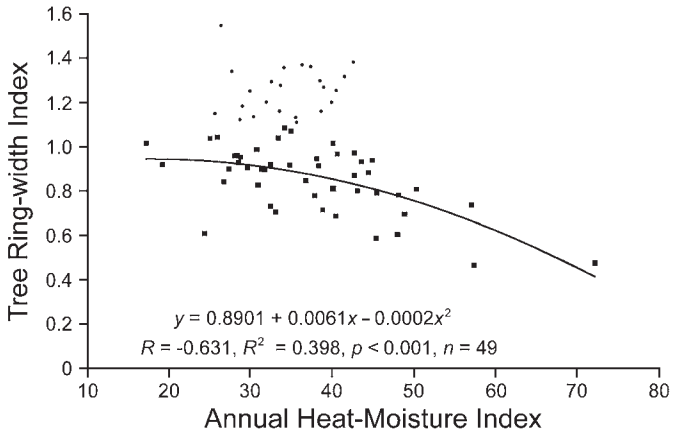

FIG. 6. Relationship between annual heat-moisture index and tree ring-width index values lower than 1.1 in the Takhini Valley based on 1942–2013 meteorological data (Environment Canada, 2016). Data points represented by small dots (as opposed to squares) were excluded from the regression analysis.

latter explaining the most variance (17%). Regression analysis found no systematic trend between RWI values and total annual precipitation. RWI values lower than 1.1 curvilinearly declined with increasing AHMI values (i.e., a negative relationship, Fig. 6), with the regression model explaining ~40% of the variance in RWI values. RWI values above 1.1 had AHMI values between 25 and 45. RWI values were not correlated ($p > 0.05$) with any of the tested climate variables during the year prior to growth of the tree-rings.

DISCUSSION

Interpretation of Chronology

The fact that temperatures (except September minima) were uncorrelated with western white spruce RWI values and precipitation was only weakly correlated (i.e., < 9% variance explanation) precluded the use of these variables to reconstruct pre-1942 Takhini Valley climate conditions. In addition, tree-ring growth is not solely a physiological function of either heat or moisture availability, but rather related to their synergistic effect (e.g., Nelson, 2011:45). The single significant and positive temperature correlation represents a spurious result or indicates that a warmer September temperature can prolong the duration of the summer ring-growth season (Oberhuber et al., 2014). The positive correlation of annual and early to mid-summer precipitation with RWI values suggests that these variables were frequently more critical in determining the amount of ring-growth than temperatures in the Takhini Valley. Greater dependence on the balance between heat and moisture availability provided a basis for interpreting the tree-ring chronology. The greater constraint of moisture availability on spruce radial growth in northwestern North America has been previously recognized by Chavardès et al. (2013) in the western Takhini Valley, as well as at various locations in Yukon (Griesbauer and Green, 2012), central Alaska (Barber et al., 2004), and northwestern Northwest Territories (Szeicz and MacDonald, 1996). The lack of correlation between Takhini Valley RWI values and temperatures was contrary to the results reported by Davi et al. (2003) and Youngblut and Luckman (2008), who analyzed sites near the tree line in the southern Yukon. For these two studies, "tree line" might be more appropriately referred to as "forest line," which is the uppermost elevation limit of forest growth, as opposed to the climatic limit of tree growth that corresponds with the lower limit of alpine ecosystems. The ecological gap between these limits in the northern British Columbia to Alaska region is occupied by subalpine shrublands that sometimes included scattered conifer trees (Meidinger and Pojar, 1991; Strong, 2013). Because forest-line sites are cooler and moister than valley bottoms, ring growth at higher elevations is more dependent upon warmer conditions than on moisture availability. However, Davi et al. (2003) and D'Arrigo et al. (2004) also noted that high-elevation spruce became less sensitive to warming summer temperatures after 1970. This fact suggests that moisture availability became a more critical constraint, and it implies that tree-ring growth in valley bottoms may also have become more moisture limited, possibly at a somewhat earlier date (see Other Chronologies section).

If annual total precipitation throughout the Takhini Valley chronology were relatively consistent (Mendoza et al., 2010: Fig. 8; Mekis and Vincent, 2011: Fig. 12) or increased slightly (e.g., 6%, Streicker, 2016), then long-term temporal differences in AHMI values would be a function of changing temperatures. This relationship would imply that mid- to late-19th century RWI increases in the second segment of the chronology were largely the result of climate warming, which created increasingly more favorable growing conditions. It would also be consistent with the gradual warming of temperatures near the end of and after the Little Ice Age (AD 1450–1850, IPCC, 2013). Mendoza et al. (2010: Fig. 6, TCM2 model) estimated

that in the Northern Hemisphere, annual temperatures for 1795–1823 and 1880–1930 were 0.37˚C and 0.31˚C below 1961–90 temperatures (Fig. 5B). The cooler of these two temperatures, in combination with a 0.92˚C increase during the last 10 years of the chronology, relative to 1961–90 (Fig. 5B), represents a baseline increase of ~1.3˚C in Takhini Valley annual temperatures. This differential, based on the median year for each of these two extreme temporal temperature estimates, represents an average increase of ~0.0645˚C per decade, which was the same as the IPCC (2013:5) increase of 0.85˚C between 1880 and 2012 (0.0644˚C per decade). Although these two estimates agree, the IPCC (2013) and Mendoza et al. (2010) values are global and Northern Hemisphere averages, respectively, and do not account for local deviations in climate. A climate reconstruction for interior Alaska found that average annual temperatures were ~2.2˚C below the 1961–90 average during the early 1800s (Jacoby and D'Arrigo, 1995). Youngblut and Luckman (2008: Fig. 3) had reconstructed early 1800s maximum June–July temperatures that were about 1.2˚C below 1961–90 averages for the same time frame. These temperatures suggest a potential range of 2.1˚–3.1˚C of warming since the early 1800s in the Takhini Valley relative to conditions that occurred during the last decade of the chronology (cf. Fig. 5B). The lower limit of this range is likely an underestimate, because average annual temperatures warmed 2˚C in Yukon after 1948 (Streicker, 2016; also see Chavardès et al., 2013:605). The doubling of RWI values also suggests that the potential for tree-ring growth has increased considerably since the early 1800s (i.e., RWI values of 0.64 versus 1.30–1.4, Fig. 5B).

The continued increase and more varied RWI values during the late 19th and early 20th centuries or second segment of the chronology than occurred earlier could signify that climate evapotranspiration demand created by ongoing atmospheric warming was beginning to exceed the moisture supply. Occurrence of the "Modern Solar Minimum" (Mendoza et al., 2010) may have dampened RWI variation during the second segment of the chronology through cooler temperatures, judging by the distinctive increase in variation after 1930 (Fig. 5B). The greater variation in post-1930 RWI values likely represents the results of continued climatic warming without a substantial increase in available moisture. Although 1950 is used as a reference date for when atmospheric greenhouse gas accumulation began to drive climate warming (IPCC, 2013), RWI variation comparable to the post-1950 period occurred about 15 years earlier in the Takhini Valley (Fig. 5B). Tree-ring chronologies presented by Allen (1982), Davi et al. (2003), and D'Arrigo et al. (2006: Fig. 5), and Youngblut and Luckman (2008) also suggest that contemporary climate warming began one or two decades before 1950 in the Yukon and Alaska portion of North America.

Concurrent Environmental Events

Several single- and multi-year RWI events occurred in the Takhini Valley chronology that were anomalous compared to the long-term trend. For example, the smallest RWI values during the first segment of the chronology (Fig. 5B) roughly corresponded with the occurrence of the Dalton Solar Minimum. If precipitation levels were similar among years in the first segment of the chronology (e.g., Mendoza et al., 2010), it could be concluded that colder conditions created by reduced solar radiation constrained tree-ring growth beyond the already cool conditions of the Little Ice Age. The last of the smallest RWI values during the first segment of the chronology occurred in 1816 and 1817, which was directly after the Tambora volcanic eruption in 1815 (Stothers, 1984). The year 1816 is known as "the year without a summer" (Stothers, 1984:1197), and post-eruption atmospheric cooling had a negative effect on ring growth in the Takhini Valley (Fig. 5B). The years 1816 and 1817 have been interpreted as moister (rather than colder) than 1815 (Cook and Krusic, 2004), which is inconsistent with a reduction in ring growth.

Other similarly low RWI values occurred in subsequent years of the chronology and were likely a response to drought rather than cold temperatures. The most notable extremes occurred in 1844–46, 1877–80, 1958, and 1998 (Fig. 5B). The locally best known of these examples is 1958 because of a major wildfire in the eastern one-third of the valley (~620 km^2 burned, Canadian Forest Service, 2003). No major wildfires occurred in the valley during 1998, but the Fox Lake fire (439 km^2 burned, Canadian Forest Service, 2003) about 60 km north of the Takhini Valley indicates that regional conditions were dry during that summer. These two years ranked 2nd and 1st, respectively, in severity with respect to AHMI values during the 1942–2013 period. The 1844–46 and 1877–80 events were also likely associated with drought conditions since major wildfires occurred immediately northwest of the study area during those years (Francis, 1996). The years 1876–78 were also associated with severe droughts in northern China, Europe, the Americas, and Southern Hemisphere continental areas (Hao et al., 2010). In comparison, the infamous 1930s Great Plains droughts of central North America (Cook et al., 2010) were represented by normal or above-normal RWI values in the Takhini Valley (Fig. 5B). Climatic conditions during the four previously indicated periods of low RWI values generally represented only slight to moderate (−1 to −2) droughts, according to reconstructed Palmer Drought Severity Index values (Cook and Krusic, 2004).

As shown in Fig. 6, below-normal RWI values are more easily explained than above-normal values with respect to AHMI values. It is difficult to explain the causal factor(s) associated with the various post-1930 RWI peaks in Fig. 5B for this reason. They did not consistently correspond with exceptional temperature or precipitation values, or with El Niño-Southern Oscillation Sea Surface Temperature,

Pacific Decadal Oscillation, or Arctic Oscillation indices. These periods of greater growth might be related more to the timing, volume, and duration of precipitation than to monthly or annual totals. Regardless of the reason, the greater RWI values represent locally maximal growth, whereas the broader deviation in values compared to pre-1930 levels suggest a more tenuous balance between moisture supply and potential evapotranspiration demand.

At a general level of comparison, the beginning and end of the second chronology segment (1840–1930, Fig. 5B) closely approximated major temporal changes in Mt. Logan (southwest Yukon) ice core $\delta^{18}O$ levels (Field et al., 2010). In the Mt. Logan chronology, a continual decline in $\delta^{18}O$ levels began in the 1840s and continued into the 1930s. Thereafter, $\delta^{18}O$ values increased until at least the year 2000. Field et al. (2010:5) interpreted the decline in $\delta^{18}O$ levels as a change in the regional atmospheric circulation pattern, with less moisture being derived from Pacific Ocean sources. The later portion and the greatest reduction in Mt. Logan $\delta^{18}O$ levels occurred during the Modern Solar Minimum (Fig. 5B).

Other Chronologies

The temporal RWI pattern in the Takhini Valley chronology most closely approximated those of the Jenny Lake and nearby Christmas Creek sites, located northwest of the study area near Kluane Lake (Zalatan and Gajewski, 2005). Most of the RWI highs and lows in the Takhini Valley also occurred in these chronologies, but the pattern and any long-term trends were more weakly represented at the Jenny Lake and Christmas Creek sites. The more extreme high and low RWI values for the Takhini Valley were evident in the chronologies developed by Chavardès et al. (2013), but their use of residual RWI values to represent the chronologies precluded identification of any long-term trend.

The regional chronology developed for the southwest Yukon region by Youngblut and Luckman (2008) contained a sequence of high and low RWI values similar to the Takhini Valley chronology, except that events in the regional chronology tended to occur 3–5 years later. This lag might be due to the greater sensitivity of low-elevation sites to changing climatic conditions. The Wrangell Mountain chronology of southeastern Alaska (Davi et al., 2003), which was similar to the Youngblut and Luckman (2008) study based on the use of forest-line sites, only roughly approximated the Takhini Valley chronology. The Takhini Valley chronology was unlike others developed farther north in Yukon (Jacoby and Cook, 1981; Szeicz and MacDonald, 1995a; Porter and Pisaric, 2011; Porter et al., 2013), nearby in the Northwest Territories (Szeicz and MacDonald, 1995b, 1996; Tomkins et al., 2008), in east-central and interior Alaska (Lloyd and Fastie, 2002; Lloyd et al., 2013), or in northern British Columbia (Flower and Smith, 2011). This lack of similarity suggests that southwest Yukon, or at least the Takhini Valley, has a climatic regime that is different from those of surrounding areas, possibly because of its location in the rain shadow of the St. Elias Mountains.

21st Century Climate Warming

Yukon has already experienced greater climate warming since the late 1940s (2˚C, Striecker, 2016) than the predicted minimum AD 2100 increase of 1˚–1.5˚C (IPCC, 2013). From an ecological perspective, continued warming will eventually allow an increase in the abundance of trembling aspen and lodgepole pine in areas where they currently exist and facilitate the western expansion of both species up the Takhini Valley. An increase of more than 10% in total annual precipitation by AD 2100 (IPCC, 2013) coupled with an even greater warming would increase general climatic aridity in an already semi-arid environment (Jätzold, 2000). To approximate the status quo, at least a 9% increase in precipitation would be required to compensate for each 1˚C increase in temperature, according to the Wang et al. (2006) annual heat-moisture index. Greater aridity would increase the frequency of wildfires (McCoy and Burns, 2005), which would further promote additional development of trembling aspen and lodgepole pine (i.e., postfire seral species) in the valley at the expense of white spruce, which is more common in older forest stands. Greater aridity might also favor expansion of grasslands, which already occur on steep southerly slopes in the Takhini Valley. The increased abundance of trembling aspen and grassland expansion could enhance foraging opportunities for wood bison (*Bison bison* Rhoads) and the struggling population of introduced elk (*Cervus canadensis* Erxleben) relative to the currently common ericaceous and feathermoss forest understory types. The enhancement of spruce growth on upland sites would occur only if effective moisture becomes more available than at present, despite the warmer conditions (Lloyd et al., 2013).

CONCLUSIONS

The results of this study indicate that RWI values in southwest Yukon forests have changed considerably during the past 200+ years. Early 19th century conditions were likely cooler and moister, with poorer tree growth than at present. Many of the lower post-1840 RWI values were likely due to ecologically drier rather than climatically colder conditions. Some of the temporal variation in the long-term Takhini Valley RWI trend relative to other nearby chronologies may represent responses to different environmental circumstances (e.g., dry warm valley bottom versus moist cool forest-line sites). Variation in the Takhini Valley chronology was too complex to be explained by a single temperature or precipitation variable and was better explained from a moisture balance perspective. The use of a large sample of scattered individual trees appears to produce RWI results similar to those derived from clustered

sets of trees judging by a limited number of pre-existing chronologies within the vicinity of the Takhini Valley. The scattered tree approach is more suited to areas where spruce stands on similar site conditions are lacking, insufficient in number, or poorly distributed to provide adequate spatial coverage of a study area. However, it is likely more labor-intensive than the conventional stand approach, because of the larger number of trees needed for a reasonable spatial representation and the greater efforts needed to measure and analyze the resulting tree-ring series.

ACKNOWLEDGEMENTS

Yukon Forest Management Branch provided access to forest cover maps. Yukon Energy, Mines and Resources Library acquired documents that were locally unavailable. B.H. Luckman (Western University, London, Ontario) provided comments on a draft of the manuscript.

REFERENCES

Allen, H.D. 1982. Dendrochronological studies in the Slims River Valley, Yukon Territory. MSc thesis, University of Calgary, Calgary, Alberta.

Barber, V.A., Juday, G.P., Finney, B.P., and Wilmking, M. 2004. Reconstruction of summer temperatures in interior Alaska from tree-ring proxies: Evidence for changing synoptic climate regimes. Climatic Change 63(1-2):91–120. https://doi.org/10.1023/B:CLIM.0000018501.98266.55

Canadian Forest Service. 2003. Yukon fire history atlas (1946–2001). Ottawa: Natural Resources Canada.

Chavardès, R.D., Daniels, L.D., Waeber, P.O., Innes, J.L., and Nitschke, C.G. 2013. Unstable climate–growth relations for white spruce in southwest Yukon, Canada. Climatic Change 116(3-4):593–611. https://doi.org/10.1007/s10584-012-0503-8

Chen, F., Zhang, Y., Shao, X., Li, M.Q., and Yin, Z.-Y. 2016. A 2000-year temperature reconstruction in the Animaqin Mountains of the Tibet Plateau, China. The Holocene 26(12):1904–1913. https://doi.org/10.1177/0959683616646187

Cook, E.R., and Krusic, P.J. 2004. North American drought atlas. Palisades, New York: Lamont-Doherty Earth Observatory and the National Science Foundation. http://iridl.ldeo.columbia.edu/SOURCES/.LDEO/.TRL/.NADA2004/.pdsi-atlas.html

Cook, E.R., Seager, R., Heim, R.R., Jr., Vose, R.S., Herweijer, C., and Woodhouse, C. 2010. Megadroughts in North America: Placing IPCC projections of hydroclimatic change in a long-term palaeoclimate context. Journal of Quaternary Science 25(1):48–61. https://doi.org/10.1002/jqs.1303

D'Arrigo, R.D., Kaufman, R.K., Davi, N., Jacoby, G.C., Laskowski, C., Myneni, R.B., and Cherubini, P. 2004. Thresholds for warming-induced growth decline at elevational tree line in the Yukon Territory, Canada. Global Biogeochemical Cycles 18: GB3021. https://doi.org/10.1029/2004GB002249

D'Arrigo, R., Wilson, R., and Jacoby, G. 2006. On the long-term context for late twentieth century warming. Journal of Geophysical Research 111, D031303. https://doi.org/10.1029/2005JD006352

Davi, N.K., Jacoby, G.C., and Wiles, G.C. 2003. Boreal temperature variability inferred from maximum latewood density and tree-ring width data, Wrangell Mountain region, Alaska. Quaternary Research 60(3):252–262. https://doi.org/10.1016/S0033-5894(03)00115-7

Drury, S.A., and Grissom, P.J. 2008. Fire history and fire management implications in the Yukon Flats National Wildlife Refuge, interior Alaska. Forest Ecology and Management 256(3):304–312. https://doi.org/10.1016/j.foreco.2008.04.040

Environment Canada. 2016. National climate data and information archive: Historical climate data. http://climate.weather.gc.ca/index_e.html

Field, R.D., Moore, G.W.K., Holdsworth, G., and Schmidt, G.A. 2010. A GCM-based analysis of circulation controls on $\delta^{18}O$ in the southwest Yukon, Canada: Implications for climate reconstruction in the region. Geophysical Research Letters 37(5), L05706. https://doi.org/10.1029/2009GL041408

Fierke, M.K., Kinney, D.L., Salisbury, V.B., Crook, D.J., and Stephen, F.M. 2005. A rapid estimation procedure for within-tree populations of red oak borer (Coleoptera: Cerambycidae). Forest Ecology and Management 215(1-3):163–168. https://doi.org/10.1016/j.foreco.2005.05.009

Flower, A., and Smith, D.J. 2011. A dendroclimatic reconstruction of June–July mean temperature in the northern Canadian Rocky Mountains. Dendrochronologia 29(1):55–63. https://doi.org/10.1016/j.dendro.2010.10.001

Francis, S.R. 1996. Linking landscape pattern and forest disturbance: Fire history of the Shakwak Trench, southwest Yukon Territory. MSc thesis, University of Alberta, Edmonton, Alberta.

Griesbauer, H.P., and Green, D.S. 2012. Geographical and temporal patterns in white spruce climate–growth relationships in Yukon, Canada. Forest Ecology and Management 267:215–227. https://doi.org/10.1016/j.foreco.2011.12.004

Grissino-Mayer, H.D., Swetnam, T.W., and Adams, R.K. 1997. The rare, old-aged conifers of El Malpais—Their role in understanding climatic change in the American Southwest. Bulletin 156. Socorro: New Mexico Bureau of Mines & Mineral Resources. 155–161.

Hao, Z.X., Zheng, J.Y., Wu, G.F., Zhang, X.Z., and Ge, Q.S. 2010. 1876–1878 severe drought in North China: Facts, impacts and climatic background. Chinese Science Bulletin 55(26):3001–3007. https://doi.org/10.1007/s11434-010-3243-z

IPCC (Intergovernmental Panel on Climate Change). 2013. Climate change 2013: The physical science basis, Technical summary. Cambridge, United Kingdom: Cambridge University Press. http://www.ipcc.ch/report/ar5/wg1/

Jacoby, G.C., and Cook, E.R. 1981. Past temperature variations inferred from a 400-year tree-ring chronology from Yukon Territory, Canada. Arctic and Alpine Research 13(4):409–418. https://doi.org/10.2307/1551051

Jacoby, G.C., and D'Arrigo, R.D. 1995. Tree ring width and density evidence of climatic and potential forest change in Alaska. Global Biogeochemical Cycles 9(2):227–234. https://doi.org/10.1029/95GB00321

Jätzold, R. 2000. Semi-arid regions of the boreal zone as demonstrated in the Yukon basin. Erdkunde 54(1):1–19. https://doi.org/10.3112/erdkunde.2000.01.01

LaMarche, V.C., Jr. 1974. Paleoclimatic inferences from long tree-ring records. Science 183(4129):1043–1048.

Lloyd, A.H., and Fastie, C.L. 2002. Spatial and temporal variability in the growth and climate response of treeline trees in Alaska. Climatic Change 52(4):481–509. https://doi.org/10.1023/A:1014278819094

Lloyd, A.H., Duffy, P.A., and Mann, D.H. 2013. Nonlinear responses of white spruce growth to climate variability in interior Alaska. Canadian Journal of Forest Research 43(4):331–343. https://doi.org/10.1139/cjfr-2012-0372

McCoy, V.M., and Burns, C.R. 2005. Potential alteration by climate change of the forest-fire regime in the boreal forest of central Yukon Territory. Arctic 58(3):276–285. https://doi.org/10.14430/arctic429

Meidinger, D., and Pojar, J. 1991. Ecosystems of British Columbia. Special Report Series 6. Victoria: British Columbia Ministry of Forests.

Mekis, E., and Vincent, L.A. 2011. An overview of the second generation adjusted daily precipitation dataset for trend analysis in Canada. Atmosphere-Ocean 49(2):163–177. https://doi.org/10.1080/07055900.2011.583910

Melvin, T.M., and Briffa, K.R. 2013. CRUST: Climatic Research Unit standardization program documentation. Norwick, United Kingdom: University of East Anglia. https://crudata.uea.ac.uk/cru/software/crust/

———. 2014a. CRUST: Software for the implementation of Regional Chronology Standardisation: Part 1. Signal-free RCS. Dendrochronologia 32(1):7–20. https://doi.org/10.1016/j.dendro.2013.06.002

———. 2014b. CRUST: Software for the implementation of Regional Chronology Standardisation: Part 2. Further RCS options and recommendations. Dendrochronologia 32(4):343–356. https://doi.org/10.1016/j.dendro.2014.07.008

Mendoza, V.M., Mendoza, B., Garduño, R., and Adem, J. 2010. Simulation of the surface temperature anomalies in the Northern Hemisphere during the last 300 years of the Little Ice Age using a thermodynamic model. Climate Research 43(3):263–273. https://doi.org/10.3354/cr00938

Miller, R.G., Jr. 1966. Simultaneous statistical inferences. New York: McGraw-Hill Book Company.

Miyamoto, Y., Griesbauer, H.P., and Green, D.S. 2010. Growth responses of three coexisting conifer species to climate across wide geographic and climate ranges in Yukon and British Columbia. Forest Ecology and Management 259(3):514–523. https://doi.org/10.1016/j.foreco.2009.11.008

Morimoto, D.S. 2015. Dendroclimatic studies of white spruce in the Yukon Territory, Canada. PhD thesis, Western University, London, Ontario. http://ir.lib.uwo.ca/etd/2991

Nehrbass-Ahles, C., Babst, F., Klesse, S., Nötzli, M., Bouriaud, O., Neukom, R., Dobbertin, M., and Frank, D. 2014. The influence of sampling design on tree-ring-based quantification of forest growth. Global Change Biology 20(9):2867–2885. https://doi.org/10.1111/gcb.12599

Nelson, E.A. 2011. Climate change in the Canadian boreal forest: The effect of warming, frost events, cloud cover and CO_2 fertilization on conifer tree rings. PhD thesis, University of Toronto, Toronto, Ontario.

Oberhuber, W., Gruber, A., Kofler, W., and Swidrak, I. 2014. Radial stem growth in response to microclimate and soil moisture in a drought-prone mixed coniferous forest at an inner alpine site. European Journal of Forest Research 133(3):467–479. https://doi.org/10.1007/s10342-013-0777-z

Pinard, J.-P. 2007. Wind climate of the Whitehorse area. Arctic 60(3):227–237. https://doi.org/10.14430/arctic215

Popovic, Z., and Menzies, J.G. 2006. Intensive and extensive sampling techniques used to measure genetic diversity of *Ustilago tritici*, using virulence and DNA polymorphism. Canadian Journal of Plant Pathology 28(2):197–207. https://doi.org/10.1080/07060660609507287

Porter, T.J., and Pisaric, M.F.J. 2011. Temperature-growth divergence in white spruce forests of Old Crow Flats, Yukon Territory, and adjacent regions of northwestern North America. Global Change Biology 17(11):3418–3430. https://doi.org/10.1111/j.1365-2486.2011.02507.x

Porter, T.J., Pisaric, M.F.J., Kokelj, S.V., and deMontigny, P. 2013. A ring-width-based reconstruction of June–July minimum temperatures since AD 1245 from white spruce stands in the Mackenzie Delta region, northwestern Canada. Quaternary Research 80(2):167–179. https://doi.org/10.1016/j.yqres.2013.05.004

Prokop, O., Kolář, T., Büntgen, U., Kyncl, J., Kyncl, T., Bošel'a, M., Choma, M., Barta, P., and Rybníček, M. 2016. On the palaeoclimatic potential of a millennium-long oak ring width chronology from Slovakia. Dendrochronologia 40:93–101. https://doi.org/10.1016/j.dendro.2016.08.001

Rossi, S., Deslauriers, A., Gričar, J., Seo, J.-W., Rathgeber, C.B.K., Anfodillo, T., Morin, H., Levanic, T., Oven, P., and Jalkanen, R. 2008. Critical temperatures for xylogenesis in conifers of cold climates. Global Ecology and Biogeography 17(6):696–707. https://doi.org/10.1111/j.1466-8238.2008.00417.x

Schmidt, R.A., Kaufmann, M.R., Porth, L., and Watkins, R.K. 1996. Measuring tree-ring increments on tree bole sections with a video-based robotic positioner. Tree Physiology 16(10):865–870.

Speer, J.H. 2010. Fundamentals of tree-ring research. Tucson: University of Arizona Press.

Stothers, R.B. 1984. The great Tambora eruption in 1815 and its aftermath. Science 224(4654):1191–1198. https://doi.org/10.1126/science.224.4654.1191

Streicker, J. 2016. Yukon climate change indicators and key findings 2015. Whitehorse: Northern Climate Exchange, Yukon Research Centre, Yukon College.

Strong, W.L. 2013. Ecoclimatic zonation of Yukon (Canada) and ecoclinal variation in vegetation. Arctic 66(1):52–67. https://doi.org/10.14430/arctic4266

Strong, W.L, and Hills, L.V. 2006. Taxonomy and origin of present-day morphometric variation in *Picea glauca* (×*engelmannii*) seed-cone scales in North America. Canadian Journal of Botany 84(7):1129–1141. https://doi.org/10.1139/b06-071

Szeicz, J.M., and MacDonald, G.M. 1995a. Dendroclimatic reconstruction of summer temperatures in northwestern Canada since A.D. 1638 based on age-dependent modeling. Quaternary Research 44(2):257–266. https://doi.org/10.1006/qres.1995.1070

———. 1995b. Recent white spruce dynamics at the subarctic alpine treeline of north-western Canada. Journal of Ecology 83(5):873–885. https://doi.org/10.2307/2261424

———. 1996. A 930-year ring-width chronology from moisture-sensitive white spruce (*Picea glauca* Moench) in northwestern Canada. The Holocene 6(3):345–351. https://doi.org/10.1177/095968369600600309

Szymczak, S., Hetzer, T., Bräuning, A., Joachimski, M.M., Leuschner, H.-H., and Kuhlemann, J. 2014. Combining wood anatomy and stable isotope variations in a 600-year multi-parameter climate reconstruction from Corsican black pine. Quaternary Science Reviews 101:146–158. https://doi.org/10.1016/j.quascirev.2014.07.010

Thornthwaite, C.W. 1948. An approach toward a rational classification of climate. Geographical Review 38(1):55–94. https://doi.org/10.2307/210739

Tomkins, J.D., Lamoureux, S.F., and Sauchyn, D.J. 2008. Reconstruction of climate and glacial history based on a comparison of varve and tree-ring records from Mirror Lake, Northwest Territories, Canada. Quaternary Science Reviews 27(13-14):1426–1441. http:dx.doi.org/10.1016/j.quascirev.2008.04.012

Wang, T., Hamann, A., Yanchuk, A., O'Neill, G.A., and Aitken, S.N. 2006. Use of response functions in selecting lodgepole pine populations for future climates. Global Change Biology 12(12):2404–2416. https://doi.org/10.1111/j.1365-2486.2006.01271.x

Yamaguchi, D.K. 1991. A simple method for cross-dating increment cores from living trees. Canadian Journal of Forest Research 21(3):414–416. https://doi.org/10.1139/x91-053

Yang, B., Qin, C., Wang, J., He, M., Melvin, T.M., Osborn, T.J., and Briffa, K.R. 2014. A 3,500-year tree-ring record of annual precipitation on the northeastern Tibetan Plateau. Proceedings of the National Academy of Sciences 111(8):2903–2908. https://doi.org/10.1073/pnas.1319238111

Youngblut, D., and Luckman, B. 2008. Maximum June–July temperatures in the southwest Yukon over the last 300 years reconstructed from tree rings. Dendrochronologia 25(3):153–166. https://doi.org/10.1016/j.dendro.2006.11.004

Yukon Forest Management Branch. 2010. Spruce bark beetle. Pamphlet 19. Whitehorse: Yukon Energy, Mines and Resources. 20 p.

Zalatan, R., and Gajewski, K. 2005. Tree-ring analysis of five *Picea glauca*-dominated sites from the interior boreal forest in the Shakwak Trench, Yukon Territory, Canada. Polar Geography 29(1):1–16. https://doi.org/10.1080/789610162